CHALMERS

Chalmers Publication Library

Modulation formats for multi-core fiber transmission

This document has been downloaded from Chalmers Publication Library (CPL). It is the author´s version of a work that was accepted for publication in:

Optics Express

Citation for the published paper:
Puttnam, B. ; Eriksson, T. ; Delgado Mendinueta, J. et al. (2014) "Modulation formats for multi-core fiber transmission". Optics Express, vol. 22(26), pp. 32457-32469.

http://dx.doi.org/10.1364/OE.22.032457

Downloaded from: http://publications.lib.chalmers.se/publication/210993

Notice: Changes introduced as a result of publishing processes such as copy-editing and formatting may not be reflected in this document. For a definitive version of this work, please refer to the published source. Please note that access to the published version might require a subscription.

Chalmers Publication Library (CPL) offers the possibility of retrieving research publications produced at Chalmers University of Technology. It covers all types of publications: articles, dissertations, licentiate theses, masters theses, conference papers, reports etc. Since 2006 it is the official tool for Chalmers official publication statistics. To ensure that Chalmers research results are disseminated as widely as possible, an Open Access Policy has been adopted.
The CPL service is administrated and maintained by Chalmers Library.

(article starts on next page)

Modulation formats for multi-core fiber transmission

B. J. Puttnam,[1] T. A. Eriksson,[2] J.-M. Delgado Mendinueta,[1] R. S. Luís,[1] Y. Awaji,[1] N. Wada,[1] M. Karlsson,[2] and E. Agrell,[3]

(1) National Institute of Information & Communications. Technology (NICT), 4-2-1 Nukui-kita, Koganei, Tokyo 184-8795, Japan.

(2) Department of Microtechnology and Nanoscience, (3) Department of Signals and Systems, Chalmers University of Technology, SE-412 96 Gothenburg, Sweden.

**ben@nict.go.jp*

Abstract: We investigate high dimensional modulation formats for multi-core fibers (MCFs) and spatial superchannels. We show that the low skew variations between MCF cores maybe exploited to generate 'multi-core' formats that offer significant advantages over independently transmitting conventional 4-dimensional formats in each core. We describe how pulse position modulation formats may be transposed to the spatial domain and then investigate a family of modulation formats referred to as core-coding, one of which has the same power and spectral efficiency as polarization switched quaternary phase shift keying but with half of the optical power, potentially improving non-linear tolerance for long distance transmission, albeit at the cost of implementation challenges. Finally, we investigate the application of set-partitioning to multi-core formats using a single-parity check bit transmitted in one quadrature of one polarization in one of the cores and polarization-division multiplexing quadrature phase shift keying data in all remaining cores. We observe that for high core counts, an advantage of almost 3 dB in asymptotic power efficiency may be obtained with negligible impact on spectral efficiency, which translates into experimentally measured reduction in the required optical signal-to-noise ratio of up to 1.8 dB at a bit-error-rate of 10^{-5} and the same data-rate, and additional transmission reach of up to 20%.

©2014 Optical Society of America

OCIS codes: (060.4080) Modulation; 060.2360 Fiber optics links and subsystems .

References and links

1. H. Takahashi, K. Igarashi, and T. Tsuritani, "Long-haul transmission using multicore fibers," In Optical Fiber Communication Conference, (Optical Society of America, technical digest 2013), paper Tu2J
2. Y. Lee, K. Tanaka, K. Hiruma, E. Nomoto, T. Sugawara, and H. Arimoto, "Experimental demonstration of a highly reliable multicore-fiber-based optical network," IEEE Photon. Technol. Lett. **26** (6), 538-540 (2014.)
3. J. Sakaguchi, B. J. Puttnam, W. Klaus, Y. Awaji, N. Wada, A. Kanno, T. Kawanishi, K. Imamura, H. Inaba, K. Mukasa, R . Sugizaki, T. Kobayashi, and M. Watanabe, "305 Tb/s space division multiplexed transmission using homogeneous 19-core fiber," IEEE J. Lightwave Technol. **31** (4), 554 - 562 (2013.)
4. R. Ryf, S. Randel, N. K. Fontaine, M. Montoliu, E. Burrows, S. Corteselli, S. Chandrasekhar, A. H. Gnauck, C. Xie, R.-J. Essiambre, P. J. Winzer, R. Delbue, P. Pupalaikis, A. Sureka, Y. Sun, L. Gruner-Nielsen, R. V. Jensen, and R. Lingle Jr., "32-bit/s/Hz spectral efficiency WDM transmission over 177-km few-mode fiber," In Optical Fiber Communication Conference, (Optical Society of America, technical digest 2013), PDP5A.1
5. M. D. Feuer, L. E. Nelson, K. Abedin, X. Zhou, T. F. Taunay, J. F. Fini, B. Zhu, R. Isaac, R. Harel, G. Cohen, and D. M. Marom "ROADM system for space division multiplexing with spatial superchannels," In Optical Fiber Communication Conference, (Optical Society of America, technical digest 2013), PDP5B.8
6. N. Amaya, S. Yan, M. Channegowda, B. R. Rofoee, Y. Shu, M. Rashidi, Y. Ou, E. Hugues-Salas, G. Zervas, R. Nejabati, D. Simeonidou, B.J. Puttnam, W. Klaus, J. Sakaguchi, T. Miyazawa, Y. Awaji, H.

Harai, and N. Wada, “Software defined networking (SDN) over space division multiplexing (SDM) optical networks: Features, benefits and experimental demonstration,” Opt. Express **22**, 3638–3647 (2014.)

7. M .D. Feuer, L. E Nelson, X. Zhou, S. L.Woodward, R. Isaac, B. Zhu, T. F. Taunay, M. Fishteyn, J. M. Fini, and M. F. Yan, “Joint digital signal processing receivers for spatial superchannels” IEEE Photon. Technol. Lett. **24**, 1957–1960 (2012.)
8. E. Agrell and M. Karlsson, “Power-efficient modulation formats in coherent transmission systems ,” IEEE J. Lightwave Technol. **27** (22), 5515-5126 (2009.)
9. M. Karlsson and E. Agrell, “Which is the most power-efficient modulation format in optical links?,” Opt. Exp. **17** (13), 10814-19 (2009.)
10. J. Pierce, “Optical channels: Practical limits with photon counting,” IEEE Trans. Comm. **26**, 1819–1821 (1978.)
11. A. J. Philips, R.A. Cryan and J.M. Senior, “Performance evaluation of optically pre-amplified PPM Systems,” IEEE Photon. Technol. Lett. **6** (5), 651-653 (1994.)
12. H. Sugiyama and K. Nosu, “MPPM: A method for improving the band-utilization efficiency in optical PPM,” IEEE J. Lightwave Technol. **7** (3), 465-472 (1989.)
13. M. Noshad and M. Brandt-Pearce, “Expurgated PPM using symmetric balanced incomplete block designs,” IEEE Commun. Lett. **16** (7), 968–971 (2012.)
14. M. Karlsson and E. Agrell, "Generalized pulse-position modulation for optical power-efficient communication," in 37th European Conference and Exposition on Optical Communications, OSA Technical Digest (Optical Society of America 2011) paper Tu.6.B.6.
15. X. Liu, T. Wood, R. Tkach, and S. Chandrasekhar, “Demonstration of record sensitivity in an optically pre-amplified receiver by combining PDM-QPSK and 16-PPM with pilot-assisted digital coherent detection,” In Optical Fiber Communication Conference, (Optical Society of America, technical digest 2011) PDPB.1
16. A. Ludwig, M. Schulz, P. Schindler, K. Kuder, S. Wolf, C. Koos, W. Freude, and J. Leuthold, "Stacking modulation formats for highest-sensitivity," in Advanced Photonics for Communications, OSA Technical Digest (online) (Optical Society of America, 2014), paper JM2B.2.
17. J. H. B. Nijhof, “Generalized L-out-of-K pulse position modulation for improved power efficiency and spectral efficiency,” In Optical Fiber Communication Conference, (Optical Society of America, technical digest 2012), paper OW3H.7
18. T. A. Eriksson, P. Johannisson, B. J. Puttnam, E. Agrell, P. A. Andrekson, and M. Karlsson, "K-Over-L multidimensional position modulation." IEEE J. Lightwave Technol, **32** (12), 2254-2262 (2014)
19. T. A. Eriksson, P. Johannisson, E. Agrell, P. A. Andrekson, and M. Karlsson, “Frequency and polarization switched QPSK,” in Proceedings of the European Conference on Optical Communications (ECOC 2013), paper Th.2.D.4
20. I. B. Djordjevic, M. Arabaci, L. Xu, and T. Wang, “Spatial-domain-based multidimensional modulation for multi-Tb/s serial optical transmission,” Opt. Express **19** (7), 6845-57 (2011.)
21. D. S. Millar, T. Koike-Akino, S. Ö Arik, K. Kojima, K. Parsons, T. Yoshida, and T. Sugihara, “High-dimensional modulation for coherent optical communications systems,” Opt. Express, **22** (7), 8798-8812 (2014.)
22. G. Ungerboeck, “Channel coding with multilevel/phase signals,” IEEE Trans. on Info. Theory 28, 55–67 (1982.)
23. L. D. Coelho and N. Hanik, “Global optimization of fiber-optic communication systems using four-dimensional modulation formats,” in Proceedings of the European Conference on Optical Communications (ECOC 2011) paper Mo.2.B.4
24. T. A. Eriksson, M. Sjödin, P. Johannisson, P.A. Andrekson, and M. Karlsson, “Comparison of 128-SP-QAM and PM-16QAM in long-haul WDM transmission,” Opt. Express **21** (16), 19269-19279 (2013.)
25. M. Sjödin, P. Johannisson, J. Li, E.Agrell, P. A. Andrekson, and M. Karlsson, “Comparison of 128-SP-QAM with PM-16-QAM,” Opt. Express **20** (8), 8356-8366 (2012.)
26. B. J. Puttnam, J.-M. Delgado Mendinueta, R. S. Luís, W. Klaus, J. Sakaguchi, Y. Awaji, N. Wada, T. A. Eriksson, E. Agrell, P. A. Andrekson, and M. Karlsson, “Energy efficient modulation formats for multi-Core fibers,” in Proceedings of OptoElectronics and Communications conference, 2014, paper WE9B-1
27. B. J. Puttnam, J.-M. Delgado Mendinueta, R. S. Luís, T. A. Eriksson, Y. Awaji, N. Wada, and E. Agrell, “Single parity check multi-core modulation for power efficient spatial super-channels,” in Proceedings of the European Conference on Optical Communications (ECOC 2014), paper MO.3.3.5
28. R. S.Tucker, “Green Optical Communications—Part I: Energy limitations in transport,” IEEE J. Lightwave Technol. **17** (2), 245-260 (2011.)
29. P. Poggiolini, A. Carena, V. Curri, G. Bosco, and F. Forghieri, “Experimental demonstration of a highly reliable multicore-fiber-based optical network,” IEEE Photon. Technol. Lett. 23 (11), 742-744 (2011.)

1. Introduction

Space-division multiplexing (SDM) using multi-core fiber (MCF) is one solution to meet the expected capacity demand for future data services being proposed for use in both long haul amplified transmission [1] and for short range links in access networks and data-centres [2]. The recent advancement in SDM technology, including fibers with up to 19 cores [3] or 6 spatial modes per polarization [4], have opened the prospect of using spatial channels to increase the dimensionality of modulation formats. Spatial channels allow multi-dimensional modulation formats that may be compatible with spatial super-channels [5], recently proposed to simplify switching and used in demonstrations of flexible SDM networks [6] by exploiting the relative uniformity of parallel spatial channels [7].

Such formats are of interest to optical transmission systems since they may offer desirable features such as improved theoretical sensitivity, as denoted by the asymptotic power efficiency (APE) at high optical signal-to-noise-ratio (OSNR), or the spectral efficiency (SE), which indicates the achievable bit-rate for a given available bandwidth [8, 9]. The APE, subsequently denoted as γ, is defined for an additive white Gaussian noise channel as $\gamma=d_{min}^2 \log_2 M/(4E_S)$, where M is the number of constellation points, E_S is the symbol energy, d_{min} is the minimum Euclidian distance between 2 symbols and the factor of ¼ normalizes the expression to be 1 for binary phase shift keying (BPSK) and quaternary phase shift keying (QPSK). The SE is defined per dimension pair as $SE=\log_2 M/(N_D/2)$, where N_D is the total number of dimensions including quadratures and polarizations. In general, it is desirable to maximize both SE and APE in an attractive format but in practice the sensitivity and SE are often traded to some extent.

In single core transmission, the most common technique for increasing the dimensionality of the 4-dimensional optical signal space of in-phase and quadrature dimensions of orthogonal polarizations is in the time domain. Known as pulse-position modulation (PPM), first investigated with intensity modulated data, higher dimensionality is achieved by splitting each symbol period into a frame of K pulse-slots. K is typically a power of two to encode an integer number of bits per frame, where the presence or absence of light in one [10, 11] or more [12] slots is used to encode data which may also be used in combination with existing coding techniques [13]. Subsequently, the same principle was combined with coherent quadrature amplitude modulation (QAM) [14] to further improve both γ and SE.

However, although combining QAM modulation with a single slot per frame enables record sensitivity to be achieved [15, 16], it comes at the cost of reduced SE, which may be increased by combining QAM symbols with multi-slot PPM to encode more bits in each symbol slot. Each variant of this family of modulations formats uses a different, fixed number of L pulses per frame of length K to transmit QAM symbols and in combination with QPSK or PS-QPSK has been shown capable of simultaneously increasing both the SE and γ compared to the case of transmitting QPSK or PS-QPSK in each symbol slot [17, 18]. Such formats are referred to here as K over L multi-dimensional position modulation [MDPM] since there are $\binom{K}{L}$ combinations of transmitting the pulses and the total number of bits per frame is $\log 2\binom{K}{L} + B_{QAM}L$, where B_{QAM} is the number of bits in each QAM symbol. The particular case where $L = K - 1$ is known as inverse-PPM (iPPM) or pulse-erasure modulation since the position data is modulated in the absence of a QAM symbol in 1 slot. These formats are of similar complexity as conventional PPM and carry an integer number of bits per frame when K is a power of two. Combined with QPSK and K = 4 it offers a 1.25 dB increased γ over QPSK with maintained SE and for K=8 both the SE and γ may be increased over QPSK [18].

As described in [18], all variants of PPM explored by exploiting the time-domain, described may also be generalized as types of MDPM and transposed to the spatial domain and cores of a MCF. Furthermore, in addition to this space-position modulation (SPM) as with formats described in section 2 and shown in Fig. 1, each polarization may be considered

individually to give space-polarization-position modulation (SPPM) such that each core has two possible slots and it has been shown that individual position modulation over polarizations has better performance in terms of both γ and SE compared to position modulation over both orthogonal polarization states [14, 18]. In addition to PPM, 8-dimensional modulation has also been experimentally demonstrated using optical frequencies [19] and simulated as modes of a multi-mode fiber [20]. Furthermore, up to 24 dimensions have been mapped on to 4D optical carriers using a PPM like structure [21].

Another technique applied to a number of 4-D formats to allow for improved γ at relatively small SE reductions is set-partitioning (SP) [22, 23]. Set-partitioning uses transmission of parity-check bits in each symbol across any number of signal dimensions to reduce the error probability of all transmitted bits and such formats have been shown to increase transmission reach compared to the polarization-division-multiplexed (PDM)-QAM formats at identical bit rates [24, 25].

Here, we compare several varieties of multi-core (MC) modulation formats both in terms of SE and γ and experimentally, showing that they can have some advantages compared to single core-formats. We describe a family of modulation formats referred to as core-coded and core-polarization coded modulation first investigated in [26], but presented here with new experimental results of a format which transmits the same γ and SE as PS-QPSK but with half of the optical power, potentially improving non-linear tolerance for long distance transmission. We then extend previous work on set-partitioned formats in an MCF using PDM-QPSK with a single-parity check (SPC) across multiple cores [27] with recirculating loop transmission experiments. We show that for high core numbers, an advantage of almost 3 dB in γ may be obtained with negligible impact on SE, which translates into experimentally measured reduction in the required OSNR of up to 1.8 dB at BER of 10^{-5} for equivalent data transmission and additional transmission reach of up to 20%. Overall these results show the potential of multi-core modulation formats to offer an additional option for improving the performance of optical transmission systems.

2. Core-coded and core-polarization coded modulation

2.1 Outline of formats

In this section, we describe a recently introduced [26] family of formats which combine QAM modulation of dimensionality D, with additional dimensions, K, of an MCF to make a 'multi-core' modulation format with total dimensionality N_D=K × D. As with MDPM formats described in the previous section, the number K is equivalent to the number of MCF cores when using a single polarization format or PDM signals in each core, but will be twice the number of cores, when using two independent single polarization signals in each core. We refer to these formats as core-coded (CC) or core-polarization coded (CPC), respectively. Each format encodes K bits in each symbol timeslot as a binary word of length K, where each bit is determined by the presence or absence of light on a core or core-polarization and we refer to these as intensity modulated (IM) bits. In addition, each illuminated core or polarization carries a QAM symbol containing B_{QAM} bits to code an average of B_{QAM}×K/2 additional bits. Hence, an average number of bits $B_{Tot} = K(1 + B_{QAM}/2)$ are encoded per MC symbol and $B_{Core} = (1 + B_{QAM}/2)$ bits encoded per core. This scheme may be considered as a variant of K-over-L-MDPM described in section 1, but with a variable number of lit cores/polarizations, as shown schematically in Fig. 1. Figure 1 also shows that compared to transmitting the same QAM format in each core or each polarization. The CC and CPC formats transmit symbols only half the time on average, meaning that the average optical power is reduced by 50%. This feature may have consequences in terms of energy consumption with energy savings at the transmitter and optical amplifiers [28], but also potentially reduces the impact of fiber nonlinearities in long, dispersive fiber links. This

follows from the well-known Gaussian noise model, according to which the nonlinear distortion is proportional to the cube of the average power [29].

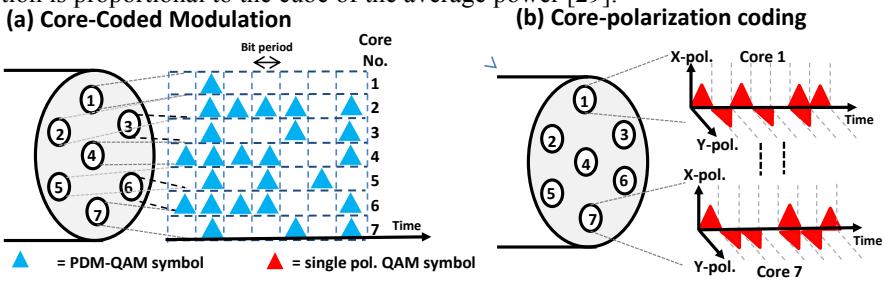

Fig. 1. Core-coding and core-polarization coded modulation.

Table 1 summarizes the SE and γ for common single-core fiber modulation formats and a comparison with the corresponding CC and CPC formats. For CC and CPC formats B_{Core} is calculated assuming each utilized spatial dimension is lit 50% of the time and $B_{Core} = B_{QAM}$ for single core formats.

Table 1: Comparison of single core QAM formats (left side) with core-coded (CC) and core and polarization-coded (CPC) formats (right side) from [26]

Format	B_{Core}	γ (dB)	SE	Format	B_{Core}	γ (dB)	SE
BPSK	4	0	2	CPC-BPSK	3	-1.25	3
PDM-BPSK	4	0	2	CC-PDM-BPSK	2	0	2
QPSK	4	0	2	CPC-QPSK	4	0	2
PDM-QPSK	4	0	2	CC-PDM-QPSK	3	1.76	1.5
PS-QPSK	4	1.76	1.5	CC-PS-QPSK	2.5	0.97	1.25

Table 1 shows that allowing a variable number of spatial channels to be lit leads to some advantages over the single core formats. However, the reduced optical power does not translate into an improved γ in most cases. CPC-BPSK offers the highest spectral efficiency of all the CC/CPC formats with a 50% increase compared to transmitting BPSK or QPSK in each core and matching the notable single core format of rectangular 8QAM. This is traded off with 1.25dB reduction in γ compared to BPSK but the γ of this format is 1.76 dB superior to 8QAM. CPC-QPSK and CC-PDM-QPSK have identical γ and SE as their single-core equivalent format but do have the potential advantage of reduced optical power. PS-QPSK appears to be better transmitted as a single core format with a reduction of both γ and SE when transmitted as CC-PS-QPSK, but CC-PDM-QPSK shows a 3dB improvement in γ at the cost of a 25% reduction in SE compared to PDM-QPSK transmission in each core. Interestingly, unlike the formats described in section 2 and 4, the SE and γ are independent of the number of cores meaning that it is also possible to implement them with multiple sets of cores in a large core count MCF or indeed a single core fiber.

2.2 Experimental investigation

The feasibility of core-coding with PDM-QAM formats was investigated experimentally using the set-up shown in Fig. 2. The set-up, improved from that [26], which only allowed single-core formats to be transmitted in each core. The improved set-up allows generation of CC and CPC formats by using Mach-Zehnder modulators (MZM) to intensity modulate one or both polarizations in each bit-slot with independent data patterns.

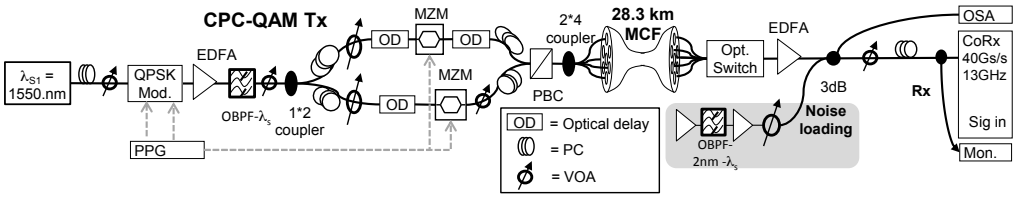

Fig. 2. Experimental set-up for CC-QAM experiments.

The optical source was an external cavity tunable laser with approximately 700 kHz linewidth and wavelength tuned to 1550 nm, modulated with a 10 GSymbol/s QPSK signal generated from a pseudo-random bit sequence (PRBS) of period 2^{15}-1 in a dual-parallel MZM, referred to subsequently and in Fig. 2 as a QPSK modulator. This signal was then amplified and filtered before being split into 2 paths in a 3dB coupler. Each path contained a MZM, driven by independent PRBS, used to pass or block the QPSK symbols with optical delays used to align the IM symbol-slots with the QPSK symbols. Polarization controllers (PCs) and variable optical attenuators (VOAs) were used to control the power and polarization into each MZM and an additional optical delay was used to align the bit-slots and decorrelate the QPSK bit-streams at the input to a polarization beam combiner (PBC). The output of the PBC was then split and connected to 4 outer cores of a 28.3 km long, 7-core fiber with average chromatic dispersion of 18 ps/nm/km, insertion loss of <0.19 dB/km and worst-case inter-core crosstalk of 36 dB/100 km. The skew variation between cores of the MCF was measured to be below 8 ps over a 24 hour period, compared to over 100 ps for the same measurement with 2 thermally isolated single core fibers of similar length.

The fiber launch power was 0 dBm, where negligible impact from fiber non-linearity was expected for single span measurements. After the fiber, an optical switch was used to select each core in turn for reception in a polarization diverse coherent optical receiver with a specific PRBS used for the measurement of each core. The coherent receiver was connected to a digital sampling oscilloscope with 13 GHz analogue bandwidth and the receiver path also contained an EDFA and a 3 dB coupler, which was used to add amplified spontaneous emission noise from filtered EDFA outputs, to enable BER measurements as a function of the OSNR. VOAs and optical taps were used to control and monitor optical power levels. A laser integrated into the receiver was used as the local oscillator for intradyne coherent detection with the signal polarization manually optimized before each acquisition, to maximize the received signal amplitude. The resulting electrical currents where then digitized at 40 GS/s. Traces were taken for each core with a common trigger for timing alignment and the receiver DSP performed offline in MATLAB. Initially, skew and chromatic dispersion compensation, normalization, multiple input-multiple output (MIMO) polarization tracking and residual carrier phase recovery were performed on the traces for each core individually before being combined for error counting. BER measurements were calculated from the average of three traces, each containing 500,000 symbols.

In practice, the variable number of bits per symbol presents new challenges for the receiver design since errors in the IM bits will change the length of the expected sequence. It is envisaged that this will require either more sophisticated bit-to-symbol mapping or for data to be sent in fixed length frames, as is currently performed to address cycle slips in commercial transmission systems. For simplicity, this was not fully addressed in this demonstration but sequences were identified by the presence of a 32 bit IM header in each PRBS sequence. We then used a simplified error counter in which the IM bits were first detected for each core and compared with the transmitted sequence. For each IM-bit error, additional errors of each QAM symbol were then added to the error total for the additional or erased QAM symbol. Finally, the QAM symbols of the correctly received 1's were then compared with the transmitted sequence to identify any remaining errors.

2.3 Experimental results and discussion

Figure 3 shows the measured and simulated BER as a function of receiver OSNR for the best performing format from Table 1, 4-CC-PDM-QPSK, where the number 4 denoted the number of signal cores used. This format is compared to PDM-QPSK simulated and generated with the same transmitter at 10 GBd in Fig. 3(a) and together with individual BERs of IM and QAM bits for each core in Fig. 3(b). The simulated line for CC-PDM-QPSK was performed by mapping a bit sequence to an alphabet of complex multi-core symbols comprising both IM and QAM bits, before simulated transmission over the additive white Gaussian noise channel. The received symbols were then decided based on the vector distance of the received multi-core symbols to the alphabet. The accumulated BER was computed by counting the bit errors of each incorrectly received symbol in turn. In this way, problems of synchronization and variable symbol lengths may be bypassed whilst allowing the d_{min} of the entire multi-core symbol to be realized, although we note that the bit-to symbol mapping used was not optimal.

Figure 3(a) shows that the MC-format has a 1dB improvement in the measured required OSNR compared to PDM-QPSK although the additional MZMs used in the transmitter mean that a 0.7dB implementation penalty is measured for PDM-QPSK compared to simulation. However, the CC-PDM-QPSK line is 1.2 dB worse than that predicted by simulation and that which could be expected from 3dB γ improvement. This is primarily a result of the simplified receiver structure used to process the experimental data. Since each core was processed individually, the receiver did not consider the entire-multi-core symbol in the setting of decision thresholds and instead the core-coding received on an individual core becomes an on-off keying or intensity modulated envelope on top of the PDM-QPSK which subsequently dominates required OSNR of the multi-core format. This is evident from considering the individually measured BERs of the QAM bits and IM bits also shown in Fig. 3(b). Since the average power of the QAM bits is 3dB below that of PDM-QPSK in each core the QAM bits in the core-coded symbols may be received with an OSNR lower than the simulated plot of PDM-QPSK. However, in practice these bits only contribute to the BER of the multi-core format after successful detection of the IM component. Hence, since the required OSNR to correctly detect the IM bits is several dB larger than that required to correctly detect the QAM bits, the IM errors dominate the overall BER performance in this implementation.

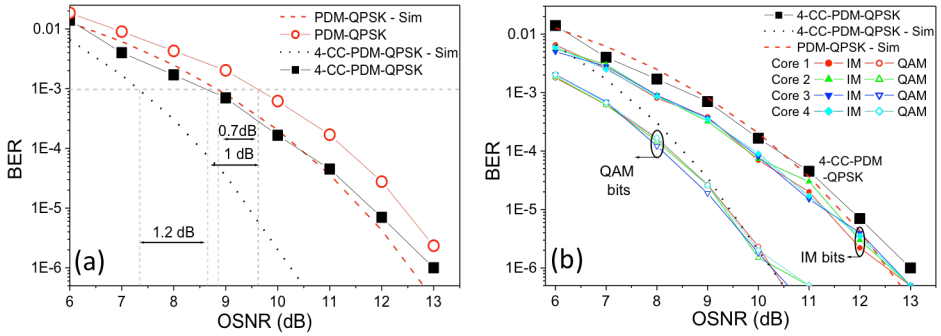

Fig. 3. Measured BER vs OSNR for (a) CC-PDM-QPSK and PDM-QPSK and (b) IM and QAM bits for 4-CC-PDM-QPSK.

These results show that although the proposed formats may offer some advantages, the receiver implementation may prevent practical use. It should be possible to reduce the OSNR requirement with improved DSP techniques using the received signals for all cores for optimal detection of the multi-core symbol instead of the 2-stage individual core approach used here. Furthermore, it may be possible that improvement can be gained from more sophisticated coding or data framing. As mentioned in the receiver description, one of the challenging features of such formats is the variable number of bits and the bit-error probability between

symbols. This means that IM errors lead to erasures and additions to the transmitted sequence that will likely require data framing. Additionally, another possibility could be to exploit error detecting codes and optimize the FEC protection for the IM bits to reduce the unequal bit error probabilities of the respective QAM and IM bits after decoding. If such coding could be applied, then the attractiveness of these formats could be greatly increased.

3. Single parity check multi-core QAM modulation

3.1 Outline of format

The four-dimensional modulation format PS-QPSK can be described as transmitting independent BPSK symbols in three dimensions, while the fourth is dependent on the other three as an SPC bit [19]. Hence, it becomes possible to extend this concept to a higher dimensionality by using spatial superchannels transmitted on MCF cores to spread the cost of the parity bit over more dimensions. In single-core transmission, set-partitioning [22-25] has been applied to QAM formats up to PDM-16QAM, transforming Gray-coded 256 symbol set of 8 bits into a 128 symbol set carrying 7 bits with the final bit maintaining parity and increasing d_{min} by a factor of $\sqrt{2}$ compared to PDM-16QAM. This format was labeled 128-SP-QAM [23], however, considering the large symbol sets possible with high core count MCFs, this naming scheme quickly becomes impractical. Instead we refer to SPC formats using multiple cores as SPC-MC-QAM modulations. Whilst, compatible with higher order QAM modulation, here, we focus on SPC-MC modulation when transmitting PDM-QPSK in each core and investigate it as a function of the number of cores.

SPC-MC-PDM-QPSK, recently investigated in [27], can be considered as transmitting independent BPSK symbols on each orthogonal polarization state up to 4K–1 dimensions of an MCF with K cores with the last reserved for the SPC bit, formed as B_{4K}=XOR(B_1, B_2,…,$B_{(4K-1)}$) where B_n is the binary or BPSK symbol in the nth dimension. This is also illustrated in Fig. 4(a), which shows the transmitter implementation based on standard PDM-QPSK modulators each with 4 binary driving bits. As with 16QAM bits, compared to PDM-QPSK, d_{min} is increased by a factor of $\sqrt{2}$ giving an advantage in γ but reducing the total number of dimensions from N_D=4K to N_D=4K-1. Hence, both the SE and γ depend on the number of available cores according as SE =2-(1/2K) and γ =2-(1/2K) although we note that the identical expression for both does not hold for higher order SPC QAM formats. The SE as a function of (1/γ) for QPSK, PDM-QPSK, PS-QPSK, and SPC-MC-PDM-QPSK with K=1,2,…,100 is shown in Fig. 4(b).

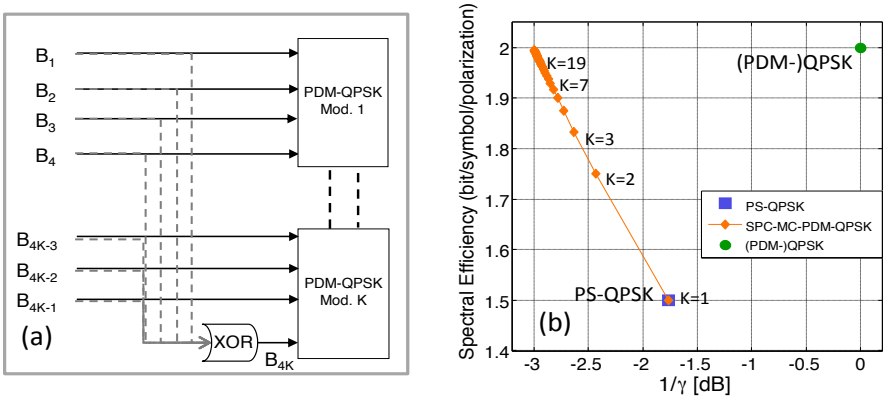

Fig. 4.(a) Logical transmitter configuration for SPC-MC-PDM-QPSK based on PDM-QPSK modulators where B_1 to B_{4K} denote binary driving bits and (b) SE as a function of asymptotic power penalty (1/γ) from [27].

Figure 4(b) shows that extending the SPC-MC-PDM-QPSK format from the single core case equivalent to PS-QPSK, leads to a simultaneous increase in both the SE and γ which for

large core number, asymptotically approaches the same SE as QPSK but with γ improved by 3 dB. For a 7-core fiber as used in experiments described here, γ is improved by 2.85dB compared to (PDM-QPSK) with the SE reduced from 2 to 1.93. For a 19-core fiber, the γ advantage over QPSK in terms of γ and SE are 2.95dB and 1.97. These results show that SPC-MC formats are interesting candidates for multi-core modulation formats.

3.2 Experimental investigation

The performance of SPC-MC-PDM-QPSK at low SNRs was investigated experimentally with measurement using both a single span of 7-core MCF, as in [26] and in a recirculating transmission experiment. The set-up for both experiments is shown in Fig. 5. A common transmitter was used for all measurements using the same laser described in Section 2.2. The light was first divided in a 3 dB coupler, with each arm containing a QAM modulator to modulate QPSK signals at a variable Baud rate before recombination on orthogonal polarizations in a PBC. An optical delay and patch cords were used to align the propagation delay in both paths, with PCs used to align the polarization before each modulator and the PBC. A VOA was used to equalize the power in both arms.

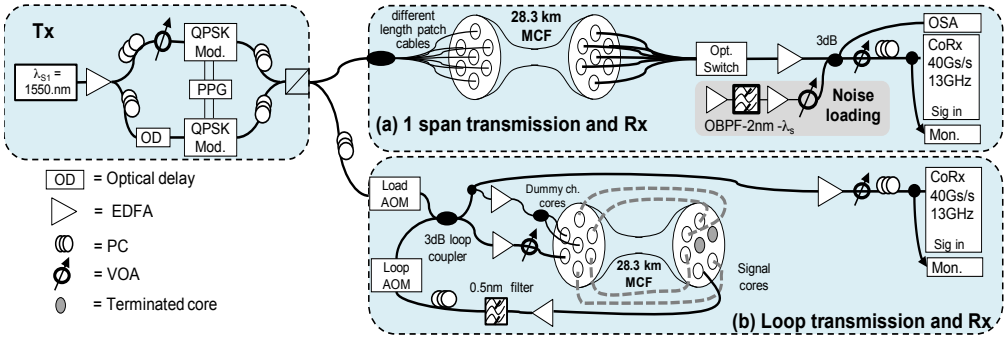

Fig. 5. Experimental set-ups for SPC-MCPDM-QPSK investigation for (a) single span and (b) recirculating transmission experiments.

For single span measurements, Fig. 5(a), the generated PDM-QPSK signal was then split between each core of the 7-core MCF described in section 2.2 with patch cables of different lengths used to decorrelate signals in each core, with all cores lit for all measurements. After the fiber, in the absence of multiple coherent receivers, an optical switch was used to select each core in turn for reception. For each multi-core format of K cores, a set of specific PRBS were generated for each core and the PPG programmed for the specific core selected before each measurement. For core numbers from 1 to K-1, four decorrelated PRBSs of period 2^{15}-1 were used for the quadrature of each polarization. For the final core (K), three of the bits were generated from additional decorrelated PRBSs, with the quadrature component of the Y polarization used for transmission of a SPC bit for the patterns in all cores of the MC-format. For all measurements, signal reception was performed in the same coherent receiver described in section 2.2 with the receiver path again allowing noise loading to enable BER measurements as a function of the OSNR.

For each core, deskewing, chromatic dispersion compensation, normalization, MIMO polarization tracking, and carrier phase recovery were performed on the traces for each core individually, before the equalized signal structures from all cores were combined for SPC bit processing and error counting. On detection of an SPC bit with odd parity, the received symbol closest to a decision threshold was identified as the most probable error and the inferred error in the transmitted stream was then corrected before error counting. All BER measurements were calculated from the average of three traces, each containing 500,000 symbols. Measurements were performed both at an equivalent symbol rate of 10 GBd and

with the clock varied between 9.375 GBd and 10.22 GBd to allow a comparison of PDM-QPSK with 3, 5, and 7 core SPC-MC-QPSK at the same bit-rate.

Finally, loop experiments were performed with the SPC format in 3 cores using the set-up shown in Fig. 5(b). Due to the short fiber span length, 2 sets of 3 fiber cores were linked together. One was used for a single core with 85km length and the second set and remaining cores used to transmit dummy channels. For simplicity, the same 3 core fiber span was used to transmit each core component of the 3-SPC-MC-PDM-QPSK format in turn with the appropriate SPC-MC patterns selected for each core. The dummy channels were generated from the loop output after each recirculation after being amplified and decorrelated with fiber patch cords. Tapping the dummy channels from the loop output ensured that they had similar noise impairment as the signal channels to more closely simulate a real MCF link. Acousto-optic modulators (AOMs) were used to control the input and recirculation time in the loop with a common timing control used to gate the AOMs and trigger the coherent receiver for reception after the required recirculation time. After the loop output, since no noise loading was required, the receiver path contained only an EDFA, PC and VOA for polarization and power control.

3.3 Experimental results and discussion

Initially, the back-to-back implementation penalty and transmission penalty were measured for each multi-core format at a fixed symbol rate. Compared to a simulation with additive white Gaussian noise as the only impairment, the implementation penalty for back-to-back transmission was under 0.3 dB, with an additional transmission penalty of 0.2 dB for all formats. For clarity, the BER as a function of OSNR for the 3 measurements is shown for 7-SPC-MC-QPSK only in Fig. 6

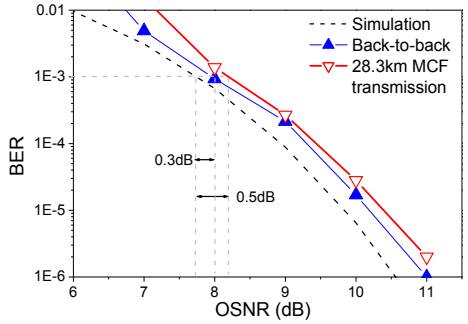

Fig. 6. Implementation and transmission penalty for 7-SPC-MC-QPSK at 10 GBd.

Figure 7(a) shows the average BER plots for the investigated formats after fiber transmission with a fixed symbol rate of 10 GBd. Compared to 10 GBd PDM-QPSK, the required OSNR for BER=1x10^{-3} is improved by 1.8, 1.3, and 1.0 dB for SPC-MC-QPSK implemented over 3, 5, and 7 cores, respectively. As may be inferred from the increased γ for the MC formats, a larger sensitivity gain is expected at high OSNR and evidence of this may be seen in the increased required OSNR advantage of the MC formats at BER of 10^{-5}, which increases to 1.8, 2.0, and 2.2 dB for 3, 5, and 7 cores, respectively. The higher required OSNR for the higher core number formats may be explained by the fact that the SPC bit is shared over a larger number of data bits. This increases the number of nearest neighbor symbols and, at low OSNRs, increases the probability of multiple errors which may remain uncorrected by the SPC bit.

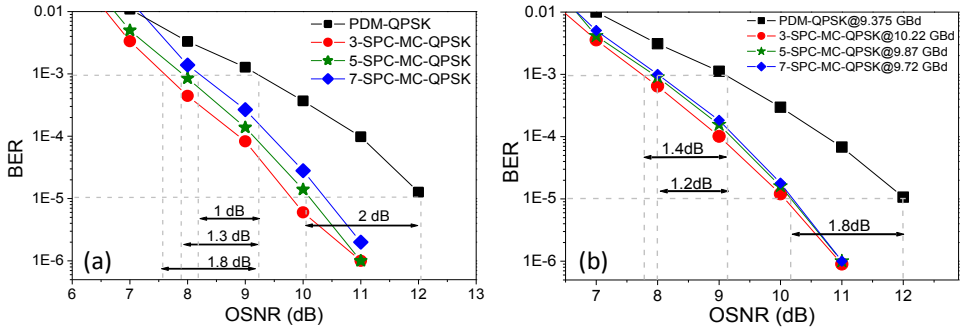

Fig. 7. BER vs OSNR for 1, 3, 5 and 7-SPC-MC-PDM-QPSK at (a) fixed symbol rate of 10Gbd and (b) equivalent bit-rate of 37.5 Gb/s per core.

The MC formats were then compared with PDM-QPSK at the equivalent bit-rate of 37.5 Gb/s per core by varying the clock rate to compensate for the different SEs of the investigated formats as shown in Fig. 7(b). At BER of 10^{-3}, the spread of the required OSNR between the MC formats reduces to 0.2 dB as the penalty resulting from increased error probability of sharing the SPC bit between more dimensions is partially compensated by the lower baud rate resulting from the increased spectral efficiency. Compared to PDM-QPSK transmission, at BER of 10^{-3}, the required OSNR is improved by 1.4, 1.3, and 1.2 dB for the 3, 5, and 7 core formats with the improvement again increasing to around 1.8 dB at BER of 10^{-5}.

Interestingly, although we measure a penalty for increasing the core number at high OSNR, the improved γ at higher core numbers should translate to improved sensitivity at even lower BERs corresponding to higher OSNRs. Specifically, γ ranges from 2.63 dB for 3 cores to 2.85 dB for 7 cores. Hence, although such low BERs cannot be measured for reasonable processing times, a BER threshold should exist where large core numbers become advantageous over smaller ones meaning that the optimum core number depends on the target BER of a specific system which could be an avenue of future study for such formats.

Finally, Fig. 8 shows the impact of implementing the multi-core format on the transmission distance obtained from recirculation loop experiments. Figure 8(a) shows the BER against transmission distance for the multi-core format across 3 cores and PDM-QPSK calculated from the average BER of the 3 cores considered individually. Fig. 8(b) shows the transmission distance for a range of launch powers for a BER=1x10^{-3}.

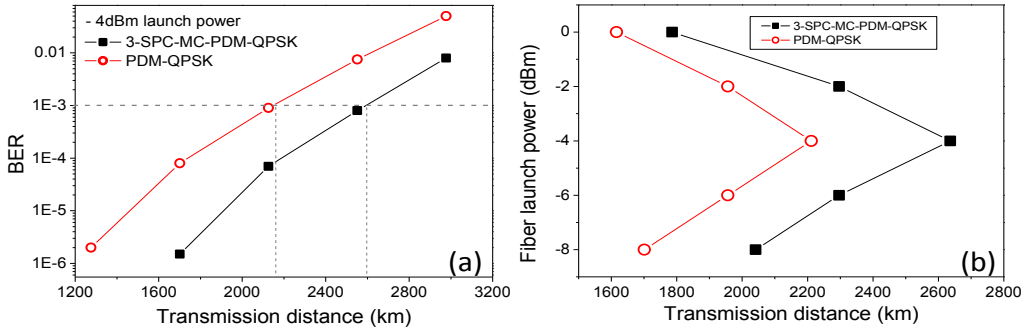

Fig. 8.(a) BER and (b) optimal fiber launch power vs transmission distance for 3-SPC-MC-PDM-QPSK at equivalent bit-rate of 37.5 Gb/s per core.

Fig. 8 shows that adopting the multi-core format with parity-bit transmission increases the transmission distance by 20% at the optimum launch power of -4 dBm with increase between 18% and 20% for other launch powers. The overall transmission distances are moderate for PDM-QPSK formats due to the large fiber loss between amplification and the accumulated

interference of MCF crosstalk in the transmission fiber. However, these results confirm that improvement in required OSNR measured in single span measurements does translate to increased transmission distance and that SPC-MC formats is compatible with long distance MCF transmission.

4. Comparison of formats

In this section, we compare the formats investigated with existing single-core formats that may be applicable to MCF, such as PPM variants, and common or interesting single core formats in terms of γ and SE. The single formats include (PDM)-QPSK and rectangular 8QAM which is notable for its high SE but suffers from a 3 dB γ penalty compared to QPSK. Both the SPC and MDPM formats are given for different K values, where K refers to the number of cores. Hence, the names MDPM formats are given as space-position-modulation (SPM) formats. Included are those with intensity modulation (K-SPM) and in combination with PDM and PS-QPSK as both SPM (KPPM-PDM-QPSK and KPPM-PS-QPSK) and iSPM (KiPPM-PDM-QPSK and KiSPM-PS-QPSK). Fig. 9 shows a plot of SE and asymptotic power penalty (1/γ) for the considered formats.

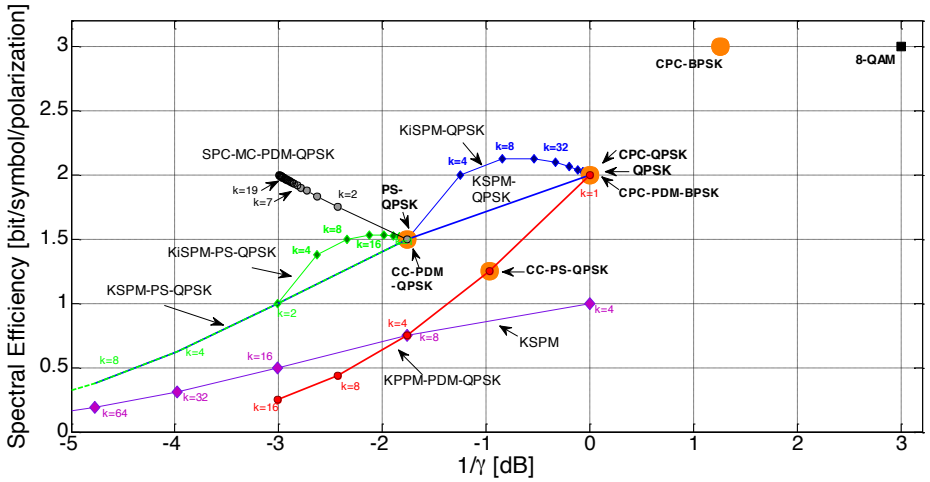

Figure 9. Spectral efficiency asymptotic power penalty $(1/\gamma)$ for SPC-MC-PDM-QPSK (grey circles), CC and CPC formats (orange circles), KSPM (purple), KSPM-PDM-QPSK (red diamond), K-SPM-QPSK (blue line), K-SPM-QPSK (blue diamonds), KSPM-PS-QPSK (green line), KiSPM-PS-QPSK(green diamonds) and single formats (black squares).

Figure 9 shows that CPC-BPSK has the same high sensitivity as 8QAM, but with a 1.76 dB improvement in γ, showing that if it could also be an interesting format if successfully implemented. The best formats in terms of power efficiency are those using KSPM, although this is clearly traded for SE, particularly for high core numbers. Both KiSPM-QPSK and KiSPM-PS-QPSK show advantages in terms of both γ and SE making them attractive multi-core formats. Of all of the formats shown in Fig. 9, perhaps the best in terms of both SE and APE are those with SPC-PDM-QPSK and these formats also showed good performance in the high SNR region with an advantage in both the required OSNR of up to 1.8dB and a 20% increase in transmission distance over the same single core format. Combined with relatively small additional complexity compared to transmitting the same independent format in each core, the SPC formats appear the most suitable MC modulation formats of those considered.

5. Conclusion

Of the formats investigated, the most appropriate for practical multi-core modulation is SPC-PDM-QPSK which has 3dB γ advantage and negligible SE reduction compared to PDM-QPSK and relatively simple implementation. Furthermore, the multi-core parity check maybe

applied to higher order QAM formats to further minimize the impact on SE. In addition to the formats described, our results show that the increasing number of spatial channels in transmission systems under research opens the way for investigation of new varieties of complex modulation formats or more sophisticated error correcting codes which may be applied to the optical signal to increase performance and potentially reduce the requirement for post-detection forward error correction. Our results also show that the relatively low skew variation between cores of a MCF make implementation and investigation of new high-dimensionality formats relatively simple compared to other forms of SDM. Overall, these results show that adopting multi-core modulation formats to increase the number of dimensions available for modulation has the potential to improve the performance of optical communications systems.

Acknowledgments
The authors thank the NICT technical staff for their assistance with the experiments described.